Acoustic Black Hole in a Stationary Hydrodynamic Flow of Microcavity Polaritons

H. S. Nguyen,[1,*] D. Gerace,[2] I. Carusotto,[3] D. Sanvitto,[4] E. Galopin,[1] A. Lemaître,[1] I. Sagnes,[1] J. Bloch,[1] and A. Amo[1]

[1]*Laboratoire de Photonique et de Nanostructures, LPN/CNRS, Route de Nozay, 91460 Marcoussis, France*
[2]*Dipartimento di Fisica, Università di Pavia, via Bassi 6, I-27100 Pavia, Italy*
[3]*INO-CNR BEC Center and Dipartimento di Fisica, Università di Trento, I-38123 Povo, Italy*
[4]*NNL, Istituto Nanoscienze - CNR, Via Arnesano, 73100 Lecce, Italy*
(Received 6 October 2014; published 22 January 2015)

We report an experimental study of superfluid hydrodynamic effects in a one-dimensional polariton fluid flowing along a laterally patterned semiconductor microcavity and hitting a micron-sized engineered defect. At high excitation power, superfluid propagation effects are observed in the polariton dynamics; in particular, a sharp acoustic horizon is formed at the defect position, separating regions of sub- and supersonic flow. Our experimental findings are quantitatively reproduced by theoretical calculations based on a generalized Gross-Pitaevskii equation. Promising perspectives to observe Hawking radiation via photon correlation measurements are illustrated.

Introduction.—Back in 1974, Hawking [1] predicted that the zero-point fluctuations of the quantum vacuum may be converted into correlated pairs of real particles at the event horizon of an astrophysical black hole. The resulting emission, called Hawking radiation, has a thermal character with a Hawking temperature T_H. Unfortunately, a direct observation of this radiation in an astrophysical context is made very difficult by the extremely low value of T_H, in the micro-K range for a solar mass black hole, well below the cosmic microwave background.

To overcome this severe limitation, a pioneering work by Unruh [2] introduced the idea of condensed-matter analogs of gravitational systems, and anticipated the occurrence of an analog Hawking emission of sound waves whenever a fluid shows an acoustic horizon separating regions of sub- and supersonic flow. Since this early prediction, intense theoretical activity was devoted to the study of different condensed-matter and optical platforms where such analog black holes could be created [3]. In the last few years, experimental realizations of horizons were reported in water channels [4], atomic Bose-Einstein condensates [5], nonlinear optical fibers [6] and silica glass [7] illuminated by strong laser pulses, and also in bulk non-linear optical systems [8]. However, the only experimental claims of stimulated and spontaneous Hawking emission reported so far, in [4] and [7], respectively, are still being actively debated by the community [9–12]. Recently, black-hole lasing was reported in a cold atomic gas [13].

In the last decade, quantum fluids of light [14] have emerged as a promising system to study quantum hydrodynamics effects, and in particular analog black holes and Hawking radiation. Among the different optical platforms, dressed photons in semiconductor microcavities in the strong coupling regime—the so-called cavity polaritons [15]—have led to the observation of superfluidity [16] and

of the hydrodynamic nucleation of quantized vortices [17,18] and solitons [19,20] in a novel optical context. Building on these results, strategies to study acoustic Hawking emission from analog black holes in photon or polariton fluids have been recently proposed [21–25].

In this Letter, we report the experimental realization of an acoustic black hole in the hydrodynamic flow of microcavity polaritons. A stationary one-dimensional (1D) flowing polariton fluid is generated by resonant cw excitation of a microcavity device laterally patterned into a photonic wire showing a localized defect potential. At high excitation power the defect separates regions of high-density subsonic flow from low-density supersonic flow, setting up an acoustic horizon. Detailed *in situ* information on the flow is obtained from real- and momentum-space photoluminescence (PL) experiments, which show full quantitative agreement with theoretical predictions based on the generalized Gross-Pitaevskii equation of Ref. [26].

Experimental setup.—Our sample, grown by molecular beam epitaxy, consists of a GaAs λ microcavity sandwiched between top or bottom Bragg reflectors, with 26 or 30 pairs of $Ga_{0.9}Al_{0.1}As/Ga_{0.05}Al_{0.95}As$ $\lambda/4$ layers. A single 8-nm-thick $In_{0.95}Ga_{0.05}As$ quantum well is inserted at the anti-node of the confined electromagnetic field, i.e., at the center of the microcavity layer. At 10 K, the temperature of our experiments, the photon quality factor amounts to $Q \sim 33\,000$ (i.e., $\hbar\gamma \sim 0.05$ meV, γ being the photon decay rate) and the Rabi splitting is $\hbar\Omega_R \sim 3.5$ meV. The microcavity is laterally etched to form photonic wires of 400-μm length and 3-μm width. An engineered defect is created at the center of the wire by enlarging its width to 5.6 μm over a length of 1 μm [Fig. 1(a)]: the reduced lateral confinement results in a localized attractive potential for polaritons with a depth of −0.85 meV. In the considered spatial region, the detuning of the photonic wire mode from the exciton
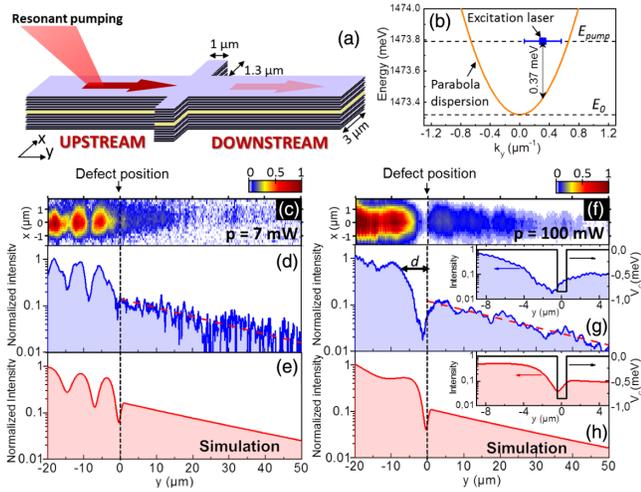
FIG. 1 (color online).   (a) Sketch of the experimental configuration. (b) Laser excitation conditions in the wave vector–energy plane. (c),(f) Linear scale image of the spatially resolved PL emission for excitation powers $p = 7$ mW and $p = 100$ mW, respectively. (d),(g) Semilogarithmic plot of the PL emission integrated over the transverse direction. Inset of (g),(h): zoom of the PL emission profile and confinement potential in the vicinity of the defect. (e),(h) Generalized Gross-Pitaevskii numerical simulation of the quantities in (d),(g).

FIG. 2 (color online).   Wave-vector-resolved PL intensity for different excitation powers. (a)–(c) Upstream region, spatially filtered from $y = -25$ μm to $y = -5$ μm. (d)–(f) Downstream region, filtered from $y = 5$ μm to $y = 50$ μm. Blue dots: experimental points; red lines: Gaussian fits.

energy is $\delta = E_{\text{cav}} - E_{\text{ex}} \approx -3$ meV, corresponding to a lower polariton effective mass 3×10^{-5} times smaller than the free electron mass.

In our experiments, a cw single-mode Ti:sapphire excitation laser is focused onto a 16-μm-wide spot 30 μm away from the defect with an angle of incidence corresponding to an in-plane wave vector $k_p = 0.3$ μm^{-1} [27]. The laser energy E_{pump} is blueshifted by 0.37 meV with respect to the (approximately) parabolic lower polariton dispersion, as shown in Fig. 1(b): as a result, polaritons ballistically propagate out of the excitation spot towards the defect [14], as schematically illustrated in Fig. 1(a). Polariton emission, collected in transmission geometry through the back of the sample, is imaged on a charge coupled device (CCD) camera coupled to a spectrometer; both real and momentum space images are acquired [27].

Low-power experiments.—The polariton flow across the defect is first characterized at low excitation power ($p = 7$ mW). In this situation, polariton-polariton interactions are negligible and the Bogoliubov dispersion of the elementary excitations in the fluid [14,26] reduces to the single-particle parabolic dispersion: backscattering from the defect is thus possible, and interference between the incoming and reflected polaritons is visible in the spatially resolved PL emission of the fluid as a strong modulation of the density pattern upstream of the defect [Fig. 1(c)]. The corresponding momentum space distribution is shown in Fig. 2(a) where the light emission from the upstream region is isolated using a spatial filter [27]: the peak at $k_y > 0$ corresponds to the incoming fluid, while the one at $k_y < 0$

is due to reflected polaritons. An analog measurement on the other side of the defect shows that the polaritons recover a ballistic flow with a single momentum space peak at $k_y > 0$ [Fig. 2(d)], while the spatial density exponentially decreases because of radiative losses [Fig. 1(d)]: the radiative lifetime estimated from the measured polariton momentum and spatial decay rate amounts to 14 ps (corresponding to $\hbar\gamma = 47$ μeV), in good agreement with the nominal sample quality factor.

High-power experiments.—As reviewed in [3], the very concept of analog models is based on the possibility of describing the wavy propagation of excitations on the fluid in terms of a curved space-time metric. In particular, this requires that excitations have a linear, soniclike dispersion on both sides of the horizon, the speed of sound then playing the role of the speed of light. While the low-density excitation spectrum has a single-particle parabolic shape, a sonic dispersion is recovered at higher densities, with a speed of sound given by $c = \sqrt{\hbar g n/m}$ in terms of the polariton-polariton interaction energy, $\hbar g$, and the polariton density, n [26,28]. In a fluid moving at velocity v, density excitations are dragged by the flow and propagate at $v \pm c$. An acoustic black-hole horizon is defined as the point where a spatially dependent flow changes from a subsonic ($v < c$) character in the upstream region to a supersonic ($v > c$) character in the downstream region: in such configurations, sonic excitations are unable to propagate back from the supersonic region to the horizon, analogous

to what happens to light trying to escape from astrophysical black holes.

In the experiment, acoustic black-hole horizons are created by increasing the laser power, so to inject a higher polariton density while keeping the same excitation geometry and laser energy. Experimental results for a 100-mW excitation power are shown in Fig. 1(f): in contrast to the low-density case, the reflection on the defect is now totally suppressed, as clearly evidenced by the absence of interference pattern in the upstream region. Correspondingly, the $k_y < 0$ peak disappears from the spatially selected momentum space data for the upstream, as shown in Fig. 2(c). As originally studied in [16,26], these features are a clear signature of the superfluid nature of the polariton fluid in the upstream region and of the subsonic character of the flow.

As shown in Fig. 1(g), the density of the polariton flow drops by a factor of ~7 over a distance $d \approx 8$ μm across the defect region, with an even deeper minimum a few μm in front of the defect. This complicated density profile is quantitatively reproduced by numerical simulations of a generalized Gross-Pitaevskii equation for the lower polariton field including pumping and loss terms [14,26] [Fig. 1(h)]. The parameters used in the simulations (potential profile, shape and energy of the pump, and losses) are directly taken from the experiment [27]. The density drop across the defect results in a corresponding decrease of the speed of sound and simultaneous increase of the flow speed, as evidenced by comparing the positions of the momentum space peaks on the two sides of the defect shown in Figs. 2(c)–2(f).

Experimental evidence of the acoustic horizon.—A quantitative insight on the subsonic vs supersonic character of the flow in the upstream or downstream region as a function of excitation power can be obtained from the momentum space pictures of Fig. 2 as follows. In our nonequilibrium stationary state, the polariton oscillation frequency is locked to the excitation laser frequency [26]. Away from the pump spot, in regions of slowly varying flow where quantum pressure is negligible, the Gross-Pitaevskii equation directly leads to a generalized Bernoulli equation for driven-dissipative polariton fluids [14],

$$E_{pump} = E_0 + \hbar^2 k_{fluid}^2/2m + E_{int}, \qquad (1)$$

where E_0 is the single-particle polariton energy at $k_y = 0$ [Fig. 1(b)], $\hbar k_{fluid}$ is the local momentum of the polariton fluid, and $E_{int} = \hbar g n$ is the interaction energy [29].

The physical meaning of this equation is visible in the momentum space data displayed in Figs. 2(a)–2(c): for the upstream region, the increase of the density with excitation power corresponds to a decreased kinetic energy; indeed, this is evidenced by the peak wave vector shifting from $k_{fluid} = 0.56$ μm^{-1} (noninteracting fluid) to $k_{fluid} = 0.21$ μm^{-1} (high power). Using Eq. (1), it is then
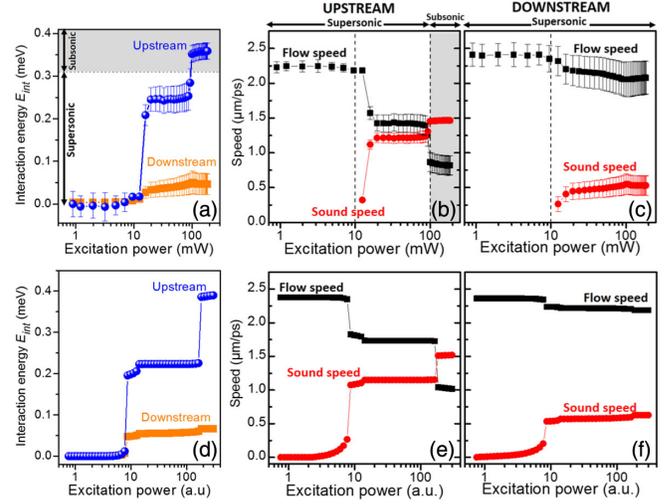
FIG. 3 (color online). (a) Interaction energy in the upstream (blue circles) and downstream (orange squares) regions as a function of excitation power. (b),(c) Flow speed and speed of sound in the (b) upstream and (c) downstream regions. (d)–(f) Results of a generalized Gross-Pitaevskii numerical simulation.

straightforward to extract from the peak wave vector, k_{fluid}, the dependence of the interaction energy on the laser excitation power. The speed of sound is directly obtained from $c = \sqrt{E_{int}/m}$. The same analysis can be done for the downstream region [Fig. 2(d)–2(f)]. The results are shown in Fig. 3. We distinguish three regimes as follows.

(1) Linear regime (for an excitation power $p < 10$ mW). In this case, $E_{int} \simeq 0$ in both upstream and downstream regions. Correspondingly, the flow speed ($v = \hbar k_{fluid}/m$), fixed by the pump frequency, is quite large and almost constant everywhere [14].

(2) Intermediate regime with supersonic-supersonic interface (for 10 mW $< p <$ 100 mW). In this case, the polariton density is large enough to have a well-defined speed of sound in both upstream and downstream regions. After a fast increase at low p, the interaction energy saturates above $p = 20$ mW. This can be explained in terms of an optical limiter behavior in the pump spot region, which sets in as soon as the interaction energy here exceeds the excitation laser detuning (0.37 meV). We note that this value of the interaction energy is large enough [$E_{int} > 2(E_{pump} - E_0)/3 \approx 0.31$ meV [27]] to give a subsonic superfluid flow under the laser spot. However, outside the excitation spot but still in the upstream region, the decrease in density caused by the radiative decay turns the fluid back into the supersonic regime with $E_{int} < 0.31$ meV [Figs. 3(a)–3(b)] in agreement with the density modulation already seen in Figs. 1(c)–1(e).

(3) Subsonic-supersonic interface. At power $p \simeq$ 100 mW, the disappearance of the density modulation is associated to an abrupt jump in the sound and flow velocities in the upstream region [Fig. 3(b)]. Indeed, the quantization of the modulation wave vector due to the

spatial confinement between the high-density region at the pump spot and the defect prevents a smooth transition.

At higher power beyond this jump ($p > 100$ mW), the flow in the upstream region rearranges itself with a lower flow speed and a high-enough interaction energy $E_{int} \approx 0.35 \pm 0.02$ meV so to have a subsonic superfluid flow up to the defect position, in agreement with the unmodulated spatial shape already seen in Fig. 1(g). On the other hand, as a consequence of the density drop at the defect position, the polariton density in the downstream region remains low enough for the flow to be supersonic [Fig. 3(c)]. The simultaneous presence of subsonic and supersonic regions on either side of the engineered defect is clear evidence of an acoustic black-hole horizon in the polariton fluid. From the quite sharp spatial profiles of the flow and sound velocities, we can anticipate a quite large analog Hawking temperature, in the Kelvin range [27].

How to detect analog Hawking emission.—Finally, we address the actual possibility of unequivocally detecting spontaneous Hawking radiation. As originally predicted in [30], the correlations between the Hawking partners can be detected in the spatially resolved, second-order density correlation function, i.e.,

$$g^{(2)}(y, y') \equiv \langle :n(y)n(y'): \rangle / [\langle n(y) \rangle \langle n(y') \rangle]. \quad (2)$$

Such a signature of the analog Hawking radiation was shown to extend to the driven-dissipative case of a polariton fluid: as fluctuations of the in-cavity polariton density are directly observable as intensity fluctuations of the emitted light, the Hawking signal can be observed in the equal-time correlations of the spatially resolved intensity noise of the emission [24].

To estimate the feasibility of such a measurement, we have performed a Wigner Monte Carlo simulation of the polariton field dynamics along the same lines of Ref. [24] with the nominal parameters of this experiment (see [27] for details). We have used the value $\hbar g = 0.3$ μeV μm for the 1D polariton-polariton interaction as extracted from another experiment on the same sample [31]. The result of an average over 2×10^5 Monte Carlo realizations is shown in Fig. 4. Correlation and anticorrelation signals are clearly visible between points belonging to different regions along the wire axis. The dashed lines indicate the points at which one would expect correlations to be strongest: compared to [32], their curved shape stems from the spatial dependence of the flow and sound velocities due to the finite polariton lifetime [27]. For the same reason, all correlation signals only extend for a finite distance from the horizon [24], which could be increased by using a higher-quality factor cavity. Finally, the additional fringes are a consequence of the curvature of the Bogoliubov dispersion and of complex density and velocity profiles in proximity to the horizon region [33].
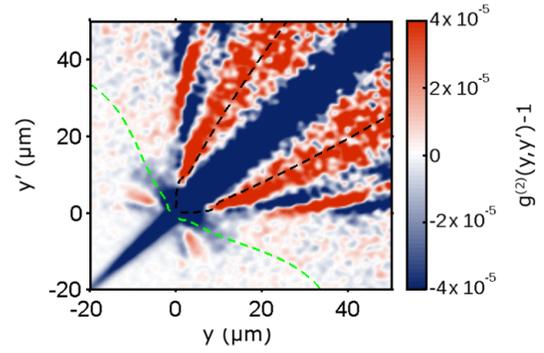
FIG. 4 (color online). Normalized spatial correlation function of photon density fluctuations, $g^{(2)}(y, y') - 1$, as predicted by an out-of-equilibrium Wigner Monte Carlo simulation [24] using the experimental parameters. A Gaussian real-space smoothing with $\ell_{av} = 1$ μm has been used.

Even if the low value of the expected correlation signal makes the experiment with the present sample quite challenging, we estimate that an integration time over ~100 h under stable experimental conditions would allow us to reach a Hawking correlation signal to noise ratio ~1 [27]. As the correlation signal scales linearly with the polariton interaction constant, the stronger (almost by an order of magnitude) interactions in wire samples with a smaller width and lower exciton-photon detuning should reduce the required integration time to ~20 min [27]; even stronger interactions are anticipated in novel cavity designs based on hybrid excitons [34] or trions [35]. In addition to optimized sample design, further promising perspectives in view of reinforcing the analog Hawking emission signal are opened by the great flexibility in generating complex polariton flows including, e.g., multihorizon configurations [33].

Conclusions.—In this Letter we have reported an experimental study of superfluid hydrodynamics of polaritons along a one-dimensional microstructure including an engineered defect. We have demonstrated the formation of an acoustic black-hole horizon. Theoretical Wigner Monte Carlo calculations show that this configuration is amenable to the detection of a Hawking radiation signal in the spatially resolved correlation function of the intensity noise of photoluminescence, a quantity directly accessible by quantum optical techniques [24,30,32].

In contrast to other analog models [4,7,10–12], our polariton fluid displays a pure acoustic black-hole horizon. As the hypotheses of the gravitational analogy are well satisfied, analog models based on polaritons offer promising perspectives as a quantum simulator for quantum field theories on a curved space-time [3,36]. Moreover, with respect to atomic systems, both the high value of T_H in the few-K range and the possibility of long integration times offered by the stationary nature of the polariton flow are promising in view of an experimental observation of the Hawking emission signal. Standard optical and

nanotechnology tools can be used to engineer the spatial shape of the horizon [37], thus reinforcing the Hawking signal [33,38]. Given this remarkable flexibility, our results suggest polariton fluids as a unique tool to study a variety of analog gravity effects in novel and tunable experimental conditions.

*hai_son.nguyen@lpn.cnrs.fr
Present address: Institut de Nanotechnologies de Lyon, Ecole Centrale de Lyon, CNRS (UMR 5270), 36 Avenue Guy de Collongue, 69134 Ecully, France.
[1] S. W. Hawking, Nature (London) **248**, 30 (1974).
[2] W. G. Unruh, Phys. Rev. Lett. **46**, 1351 (1981).
[3] C. Barceló, S. Liberati, and M. Visser, Living Rev. Relativity **8**, 12 (2005).
[4] S. Weinfurtner, E. W. Tedford, M. C. J. Penrice, W. G. Unruh, and G. A. Lawrence, Phys. Rev. Lett. **106**, 021302 (2011).
[5] O. Lahav, A. Itah, A. Blumkin, C. Gordon, S. Rinott, A. Zayats, and J. Steinhauer, Phys. Rev. Lett. **105**, 240401 (2010).
[6] T. G. Philbin, C. Kuklewicz, S. Robertson, S. Hill, F. König, and U. Leonhardt, Science **319**, 1367 (2008).
[7] F. Belgiorno, S. L. Cacciatori, M. Clerici, V. Gorini, G. Ortenzi, L. Rizzi, E. Rubino, V. G. Sala, and D. Faccio, Phys. Rev. Lett. **105**, 203901 (2010).
[8] M. Elazar, V. Fleurov, and S. Bar-Ad, Phys. Rev. A **86**, 063821 (2012).
[9] R. Schützhold and W. G. Unruh, Phys. Rev. Lett. **107**, 149401 (2011).
[10] S. Finazzi and I. Carusotto, Phys. Rev. A **89**, 053807 (2014).
[11] F. Michel and R. Parentani, Phys. Rev. D **90**, 044033 (2014).
[12] L.-P. Euvé, F. Michel, R. Parentani, and G. Rousseaux, arXiv:1409.3830.
[13] J. Steinhauer, Nat. Phys. **10**, 864 (2014).
[14] I. Carusotto and C. Ciuti, Rev. Mod. Phys. **85**, 299 (2013).
[15] C. Weisbuch, M. Nishioka, A. Ishikawa, and Y. Arakawa, Phys. Rev. Lett. **69**, 3314 (1992).
[16] A. Amo, J. Lefrère, S. Pigeon, C. Adrados, C. Ciuti, I. Carusotto, R. Houdré, E. Giacobino, and A. Bramati, Nat. Phys. **5**, 805 (2009).
[17] G. Nardin, G. Grosso, Y. Leger, B. Pietka, F. Morier-Genoud, and B. Deveaud-Pledran, Nat. Phys. **7**, 635 (2011).

[18] D. Sanvitto, S. Pigeon, A. Amo, D. Ballarini, M. D. Giorgi, I. Carusotto, R. Hivet, F. Pisanello, V. G. Sala, P. S. S. Guimarães, R. Houdré, E. Giacobino, C. Ciuti, A. Bramati, and G. Gigli, Nat. Photonics **5**, 610 (2011).
[19] A. Amo, S. Pigeon, D. Sanvitto, V. G. Sala, R. Hivet, I. Carusotto, F. Pisanello, G. Leménager, R. Houdré, E. Giacobino, C. Ciuti, and A. Bramati, Science **332**, 1167 (2011).
[20] M. Sich, D. N. Krizhanovskii, M. S. Skolnick, A. V. Gorbach, R. Hartley, D. V. Skryabin, E. A. Cerda-Méndez, K. Biermann, R. Hey, and P. V. Santos, Nat. Photonics **6**, 50 (2012).
[21] F. Marino, Phys. Rev. A **78**, 063804 (2008).
[22] I. Fouxon, O. V. Farberovich, S. Bar-Ad, and V. Fleurov, Europhys. Lett. **92**, 14002 (2010).
[23] D. D. Solnyshkov, H. Flayac, and G. Malpuech, Phys. Rev. B **84**, 233405 (2011).
[24] D. Gerace and I. Carusotto, Phys. Rev. B **86**, 144505 (2012).
[25] P-E. Larré and N. Pavloff, Europhys. Lett. **103**, 60001 (2013).
[26] I. Carusotto and C. Ciuti, Phys. Rev. Lett. **93**, 166401 (2004).
[27] See Supplemental Material at http://link.aps.org/supplemental/10.1103/PhysRevLett.114.036402 for details on the experimental setup, the measurement of the Bogoliubov dispersion, the estimation of the Hawking temperature, the theoretical treatment of the polariton fluid through the generalized Gross-Pitaevskii and Wigner Monte Carlo methods, and an estimation of the integration time necessary to detect the correlation signal of spontaneous Hawking pair emission.
[28] V. Kohnle, Y. Léger, M. Wouters, M. Richard, M. T. Portella-Oberli, and B. Deveaud-Plédran, Phys. Rev. Lett. **106**, 255302 (2011).
[29] For simplicity, we have neglected the small contribution of the polaritons in the negative k_y peak in Figs. 2(a)–2(b) (i.e., of the density modulation) to the interaction energy.
[30] R. Balbinot, A. Fabbri, S. Fagnocchi, A. Recati, and I. Carusotto, Phys. Rev. A **78**, 021603(R) (2008).
[31] H. S. Nguyen et al. (to be published).
[32] I. Carusotto, S. Fagnocchi, A. Recati, R. Balbinot, and A. Fabbri, New J. Phys. **10**, 103001 (2008).
[33] I. Zapata, M. Albert, R. Parentani, and F. Sols, New J. Phys. **13**, 063048 (2011).
[34] P. Cristofolini, G. Christmann, S. I. Tsintzos, G. Deligeorgis, G. Konstantinidis, Z. Hatzopoulos, P. G. Savvidis, and J. J. Baumberg, Science **336**, 704 (2012).
[35] S. Smolka, W. Wuester, F. Haupt, S. Faelt, W. Wegscheider, and A. Imamoğlu, Science **346**, 332 (2014).
[36] N. D. Birrell and P. C. W. Davies, *Quantum Fields in Curved Space* (Cambridge University Press, Cambridge, U.K., 1982).
[37] H. S. Nguyen, D. Vishnevsky, C. Sturm, D. Tanese, D. Solnyshkov, E. Galopin, A. Lemaître, I. Sagnes, A. Amo, G. Malpuech, and J. Bloch, Phys. Rev. Lett. **110**, 236601 (2013).
[38] S. Finazzi, F. Piazza, M. Abad, A. Smerzi, and A. Recati, arXiv:1409.8068.